Reversible Random Coil to β-Sheet Transition and the Early Stage of Aggregation of the Aβ(12−28) Fragment from the Alzheimer Peptide

Jüri Jarvet, Peter Damberg, Karl Bodell,† L. E. Göran Eriksson, and Astrid Gräslund*

Contribution from the Department of Biophysics, Arrhenius Laboratories, Stockholm University, S-106 91 Stockholm, Sweden

Received April 13, 1999. Revised Manuscript Received February 18, 2000

Abstract: The Alzheimer peptide fragment Aβ(12−28) was studied at millimolar concentration by parallel experiments with high-resolution nuclear magnetic resonance (NMR) and circular dichroism (CD) in solution at a pH close to the isoelectric point of the peptide. A preparation procedure using low temperature and low ionic strength buffer gave a sample with stable and reproducible properties. Reversible changes in secondary structure and state of aggregation were studied by variation of temperature. High-temperature promotes aggregation and β-sheet induction, whereas low-temperature shifts the equilibrium toward low molecular weight fractions and less β-sheet like structure. NMR diffusion experiments show that the dominating, most low molecular weight fraction is monomeric. With increasing temperature, residues $F_{20}A_{21}E_{22}$, overlapping with the so-called central hydrophobic segment of the Aβ peptide, exhibit the most pronounced α-proton NMR secondary chemical shift changes from random coil toward more β-sheet like structure. High ionic strength also promotes aggregation and β-sheet induction. The combined spectroscopic results, including also molecular weight estimations by cutoff filters, are summarized in a scheme in which monomeric mostly random coil and heterogeneous aggregated partly β-sheet forms of the peptide are in a temperature-dependent equilibrium, a situation which corresponds to an early stage of the fibrillogenesis.

Introduction

The amyloid β-peptide (Aβ) is a main component of the amyloid plaques found in the brain lesions of patients suffering from the Alzheimer's disease (AD).[1,2] The Aβ peptide is 39−43 residues long and is a cleavage product of a larger protein amyloid precursor protein (APP). The in vivo conditions required for the precipitation of the circulating Aβ peptides are still not understood in molecular details. Aggregation of the peptide is a prerequisite in the early state of fibrillogenesis. The aggregation process is complex and depends on hydrophobic and electrostatic interactions between the Aβ molecules, which eventually lead to a supramolecular structure with its typical amyloidic β-sheet arrangement. The properties of amyloidic matter and the processes and conditions behind the fibrillogenesis have been reviewed.[1,2] Although the amyloid deposits are very resistant, extraction of dimeric Aβ species from brains have been reported.[3,4] A stable dimeric state seems to exist also in vitro for the full length Aβ(1−40).[5−7] However, this was recently challenged[8] when, instead, a monomeric state was suggested to dominate, and also to be the active species in the growth of the plaques. The propagation of fibrils is a time- and temperature-dependent process, where particles with different aggregational states (oligomers, protofibrils, and fibrils) occur, and also become reorganized.[9,10]

Working with the full length Aβ peptides requires special precautions and preconditioning of the samples. Rather harsh treatment with acids or organic solvents has been recommended.[11] In the present study we have used the fragment Aβ-(12−28), $VHHQ_{15}KLVFF_{20}AEDVG_{25}SNK$ (M_w 1955 D), which is easier to handle. It has been reported to have amyloidic properties.[12] Whether it will deposit onto preformed plaques is not clear, since even the longer fragment Aβ(1−28) is not plaque competent, unless it is amidated.[1,13] Nevertheless, the (12−28) fragment contains residues considered to be important for the transition into β-sheet secondary structure and amyloid formation.[14] We have spectroscopically characterized the Aβ fragment,

* To whom correspondence should be addressed: Phone: +468162450. Fax: +468155597. E-mail: astrid@biophys.su.se.

† Permanent address of K. B. is Department of Medical Laboratory Sciences and Technology, Karolinska Institute, Stockholm, Sweden.

(1) Maggio, J. E.; Mantyh, P. W. *Brain Pathol.* **1996**, *6*, 147−162.

(2) Harper, J. D.; Lansbury, P. T., Jr. *Annu. Rev. Biochem.* **1997**, *66*, 385−407.

(3) Roher, A. E.; Chaney, M. O.; Kuo, Y. M.; Webster, S. D.; Stine, W. B.; Haverkamp, L. J.; Woods, A. S.; Cotter, R. J.; Tuohy, J. M.; Krafft, G. A.; Bonnell, B. S.; Emmerling, M. R. *J. Biol. Chem.* **1996**, *271*, 20631−20635.

(4) Cherny, R. A.; Legg, J. T.; McLean, C. A.; Fairlie, D. P.; Huang, X.; Atwood, C. S.; Beyreuther, K.; Tanzi, R. E.; Masters, C. L.; Bush. A. I. *J. Biol. Chem.* **1999**, *274*, 23223−23228.

(5) Garzon-Rodriguez, W.; Sepulveda-Becerra M.; Milton, S.; Glabe, C. G. *J. Biol. Chem.* **1997**, *272*, 21037−21044.

(6) Walsh, D. M.; Lomakin, A.; Benedek, G. B.; Condron, M. M.; Teplow, D. B. *J. Biol. Chem.* **1997**, *272*, 22364−22372.

(7) Kuo, Y.-M.; Emmerling, M. R.; De Lima, N.; Roher, A. E. *Biochim. Biophys. Act.* **1998,** *1406*, 291−298.

(8) Tseng, B. P.; Esler, W. P.; Clish, C. B.; Stimson, E. R.; Ghilardi, J. R.; Vinters, H. V.; Mantyh, P. W.; Lee, J. P.; Maggio, J. E. *Biochemistry* **1999**, *38*, 10424−10431.

(9) Harper, J. D.; Wong, S. S.; Lieber, C. M.; Lansbury, P. T., Jr. *Biochemistry* **1999**, 38, 8972−8980.

(10) Walsh, D. M.; Hartley, D. M.; Kusumoto, Y.; Fezoui, Y.; Condron, M. M.; Lomakin, A.; Benedek, G. B.; Selkoe, D. J.; Teplow, D. B. *J. Biol. Chem.* **1999**, *274*, 25945−25952.

(11) Jao, S.-C.; Ma, K.; Talafous, J.; Orlando, R.; Zagorski, M. G. *J. Exp. Clin. Invest.* **1997**, *4*, 240−252.

(12) Fraser, P. E.; Nguyen, J. T.; Surewicz, W. K.; Kirschner, D. A. *Biophys. J.* **1991**, *60*, 1190−1201.

(13) Lee, J. P.; Stimson, E. R.; Ghilardi, J. R.; Mantyh, P. W.; Lu, Y.-A.; Felix, A. M.; Llanos, W.; Behbin, A.; Cummings, M.; Criekinge, M. V.; Timms, W.; Maggio, J. E. *Biochemistry* **1995**, *34*, 5191−5200.

10.1021/ja991167z CCC: $19.00 © 2000 American Chemical Society
Published on Web 04/20/2000

under conditions on the borderline of fibrillation, so that reproducible and reversible observations relevant for the *early* stages of aggregation could be made. The outcome depends on many variables: Aβ concentration, temperature, pH, ionic strength, etc. In other Aβ studies, particularly those by NMR where a high concentration is desired, the peptides have been stabilized by using either a very low pH,[15,16] mixed aqueous/organic solvents,[13,17,18] detergent micelles,[19−24] or terminal blocking.[25,26] Other NMR studies have been performed around pH 5, but then with a low peptide concentration.[27,28]

In the present studies we have chosen to work at a pH close to 5, where aggregation and fibrillogenesis occur for Aβ(9−25),[29] and Aβ(10−35).[25,26] Recently[9] also strong protofibril formation was demonstrated at about pH 5 with Aβ(1−40). The isoelectric point of the full length peptide is about 5.2,[1] compared to an estimated pI ∼ 6 for Aβ(12−28). In our study of Aβ(12−28), a solvent with low ionic strength was used in order to slow down the fibrillogenesis. Dissolving the peptide up to mM concentrations directly into an ice-cold aqueous solvent with low ionic strength at pH 5, which is close to the isoelectric point of peptide, gives a sample with reproducible and stable spectral properties (on a time scale from hours to days). Identical samples in respect of concentration, salt and pH for the ^{1}H NMR and CD experiments could be employed when reversible temperature induced changes of secondary structure[30] and state of aggregation were studied.

Recent NMR diffusion studies,[15,16] using pulsed-field gradient NMR, have been performed on Aβ(12−28) at pH 2.9, with the two central F residues replaced by G, causing a monomeric form of the peptide to prevail. Preparing a disulfide-linked peptide gave a dimeric form. This work gave some basic information on the diffusion constants for the two forms of the peptide. We have performed similar diffusion measurements on Aβ(12−28) itself, but at a pH value of 5 to clarify the state of aggregation of the peptide under the present conditions. In parallel we have used molecular weight cutoff filters to obtain an estimate of the heterogeneous states of aggregation.

Table 1. Temperature-Dependent Fractions of 0.9 mM Aβ(12−28) in 10 mM Acetate-d_3 Buffer at pH 5.0[a]

temperature (°C)	fraction of sample (%) in aggregate <10 kD	10−30 kD[b]	30−100 kD[b]	>100 kD	NMR[c] % invisible	CD[d] % β-sheet
5	49	31	20	0	30	30
25	47	17	26	10	40	50
45	55	13	11	21	45	70

[a] The fractions of aggregates with different molecular weights were obtained from cutoff filtering experiments, using filters with cutoff limits at 10, 30, and 100 KD [b] Difference between fractions passing the two filters. [c] From quantitation of NMR spectra using the KKLVFFA peptide as a standard [d] From evaluation of CD spectra as a sum of random coil and β-sheet standard spectra

The results show that the early stages of aggregation and secondary structure conversion are reversible processes, which can be monitored in quantitative detail by combining the methods we have used. A scheme is presented in order to explain our observations with a minimum of assumptions. It involves a monomeric peptide fraction, in a dominating random coil conformation, which is in equilibrium with larger aggregates with heterogeneous sizes, partly in β-sheet conformation.

Results

Molecular Weight Cutoff Filtering. Molecular weight selective filters with cutoff limits at 3, 10, 30, and 100 kD were used to determine the overall states of aggregation at different temperatures in 0.9 mM solutions of Aβ(12−28), buffered at pH 5.0 with 10 mM acetate. The results (Table 1) showed that there is a considerable heterogeneity in the sample at all temperatures, with about half of the peptides in aggregates with molecular weights above 10 kD. However, the 100 kD filter was completely permeable for Aβ(12−28) at 5 °C and low salt concentration, and only slightly less permeable at the higher temperatures. A separate experiment showed that these results are strongly concentration dependent: the 10 kD filter had a constant high permeability for Aβ(12−28) at 5 °C up to about 0.3 mM concentration, but at higher concentrations the permeability went down. Furthermore, in the presence of 150 mM KF and with Aβ(12−28) concentrations as low as 0.2 mM, the 10 kD filter was almost impermeable to the peptide at 20 °C. We also studied the short peptide KKLVFFA (corresponding to Aβ(15−21) with Q_{15} replaced by K) alone at 0.9 mM and in the presence of 0.9 mM Aβ(12−28) at 5 °C and pH 5.0. In both cases, even a 3 kD cutoff filter was completely (≥90%) permeable to the small peptide (data not shown). This peptide could therefore be used as a nonaggregating quantitative standard in NMR.

CD Spectroscopy. CD spectra were recorded with a 0.9 mM Aβ(12−28) sample at low ionic strength at pH 5.0 as a function of temperature (Figure 1). The shape of the CD spectrum at 5 °C is dominated by a random coil like shape with a prominent negative band centered at 195 nm. Toward higher temperatures, the spectrum changes to less negative ellipticities at wavelengths below 200 nm, indicative of more β-sheet like secondary structure. The temperature effects seen by CD are completely reversible up to 25 °C, whereas after 30 min at 45 °C the changes in the CD spectrum were not completely reversible. For temperatures between 5 °C and 25 °C, a well-defined isodichroic point was visible in the CD spectra at 208 nm, indicating a two-state equilibrium. The CD spectra were evaluated in terms of a mixture of random coil and β-sheet

(14) Esler, W. P.; Stimson, E. R.; Ghilardi, J. R.; Vinters, H. V.; Lee, J. P.; Mantyh, P. W.; Maggio. J. E. *Biochemistry* **1996**, *35*, 749−757.
(15) Mansfield, S. L.; Jayawickrama, D. A.; Timmons, J. S.; Larive, C. K. *Biochim. Biophys. Acta* **1998**, *1382*, 257−265.
(16) Mansfield, S. L.; Gotch, A. J.; Harms, G. S.; Johnson, C. K.; Larive, C. K. *J. Phys. Chem. B* **1999**, *103*, 2262−2269.
(17) Sticht, H.; Bayer, P.; Willbold, D.; Dames, S.; Hilbich, C.; Beyreuther, K.; Frank, R. W.; Rösch, P. *Eur. J. Biochem.* **1995**, *233*, 293−298.
(18) Jayawickrama, D.; Zink, S.; Vander Velde, D.; Effiong, R. I.; Larive, C. K. *J. Biomol. Struct. Dyn.* **1995**, *13*, 229−244.
(19) Talafous, J.; Marcinowski, K. J.; Klopman, G.; Zagorski, M. G. *Biochemistry* **1994**, *33*, 7788−7796.
(20) Salomon, A. R.; Marcinowski, K. J.; Friedland, R. P.; Zagorski, M. G. *Biochemistry* **1996**, *35*, 13568−13578.
(21) Fletcher, T. G.; Keire, D. A. *Protein. Sci.* **1997**, *6*, 666−675.
(22) Marcinowski, K. J.; Shao, H.; Clancy, E. L.; Zagorski, M. G. *J. Am. Chem. Soc.* **1998**, *120*, 11082−11091.
(23) Coles, M.; Bicknell, W.; Watson, A. A.; Fairlie, D. P.; Craik, D. J. *Biochemistry* **1998**, *37*, 11064−11077.
(24) Shao, H.; Jao, S. C.; Ma, K.; Zagorski, M. G. *J. Mol. Biol.* **1999**, *285*, 755−773.
(25) Burkoth, T. S.; Benzinger, T. L. S.; Jones, D. N. M.; Hallenga, K.; Meredith, S. C.; Lynn, D. G. *J. Am. Chem. Soc.* **1998**, *120*, 7655−7656.
(26) Burkoth, T. S.; Benzinger, T. L. S.; Urban, V.; Lynn, D. G.; Meredith, S. C.; Thiyagarajan, P. *J. Am. Chem. Soc.* **1999**, *121*, 7429−7430.
(27) Zhang, S.; Casey, N.; Lee, J. P. *Folding Des.* **1998**, *3*, 413−422.
(28) Barrow, C. J.; Yasuda, A.; Kenny, P. T. M.; Zagorski, M. G. *J. Mol. Biol.* **1992**, *225*, 1075−1093.
(29) Huang, T. H. J.; Fraser, P. E.; Chakrabartty, A. *J. Mol. Biol*. **1998**, *269*, 214−224.
(30) It should be pointed out that when the terms random coil and β-sheet like secondary structure are used here, we refer to the dihedral angle structure of the individual peptide strand as revealed by spectroscopy. The state of oligomerization and aggregation is dealt with separately.

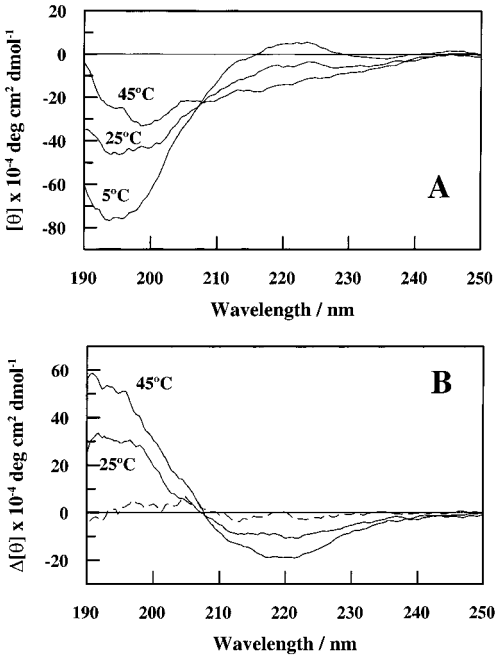

Figure 1. Circular dichroism (CD) spectra of 0.9 mM Aβ(12−28) in 10 mM acetate-d_3 buffer in D_2O at pH 5.0 (uncorrected pH meter reading). (A) The peptide was dissolved at 5 °C and spectra were recorded at 5 °C, 25 °C and 45 °C. (B) Difference spectra relative to the 5 °C spectrum. The dashed line shows the difference between two spectra recorded at 5 °C, before and after the sample was kept at 25 °C for 30 min. Difference spectra for 25 °C and 45 °C are drawn with solid lines. The CD spectra were recorded with 0.05 mm optical path length.

standard spectra with results as shown in Table 1. CD experiments were also performed with a 200 fold diluted peptide sample (5 μM at pH 5.0). At 5 °C the mean residual ellipticity at 195 nm was about a factor of 1.2 more negative (data not shown). The CD spectra recorded at increasing salt concentrations up to 20 mM KF (Figure 1S, Supporting Information), indicated an increasing salt-induced transition from a random coil state toward a more β-sheet like secondary structure.

NMR Spectroscopy. One- and two-dimensional ^{1}H NMR spectra were recorded for the 0.9 mM Aβ(12−28) sample with low ionic strength at pH 5.0 and 5 °C. Resonance assignment was performed using standard procedures.[31] Figure 2A−C shows the α-proton region of ^{1}H NMR spectra from the Aβ(12−28) peptide at 5, 25, and 45 °C. With increasing temperature the resonances broaden and some are shifted toward higher fields. The effects of a moderately high temperature were completely reversible, evidenced by an identical 5 °C spectrum recorded after 48 h at 25 °C (Figure 2S, Supporting Information). After 1 h at 45 °C, the reversibility was not quite complete (Figure 2D). The complete reversibility in the temperature-induced effects between 5 and 25 °C are in agreement with the CD results (Figure 1B, dashed line).

To determine how much of the sample concentration contributed to these NMR spectra we recorded in parallel the NMR spectra of the Aβ(12−28) and the KKLVFFA peptides, both 0.9 mM and pH 5.0. From the filtering experiment we knew that KKLVFFA did not contain any higher aggregates and we assumed that the whole concentration of this sample contributed to NMR signals and could be used as a quantitative standard. Well-separated α-proton resonances were integrated and compared for the two samples. The results showed that about 30% of the 0.9 mM Aβ(12−28) sample was invisible in the NMR spectrum at 5 °C, increasing to about 45% invisible fraction in the spectrum recorded at 45 °C (Table 1).

(31) Wüthrich, K. *NMR of Proteins and Nucleic Acids*; Wiley: New York, 1986.

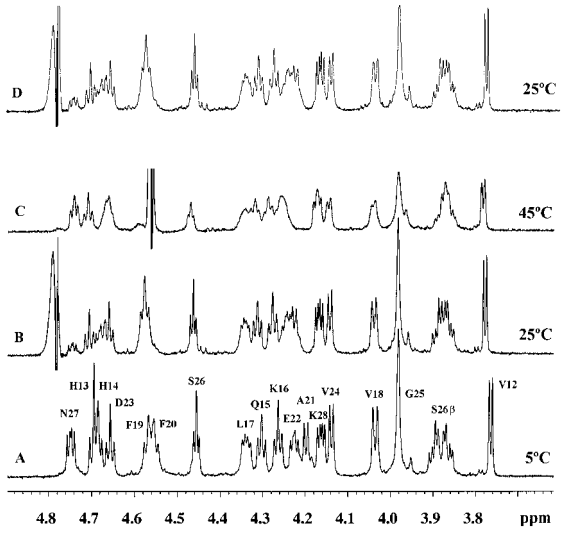

Figure 2. 800 MHz ^{1}H NMR spectra (α-proton region) of 0.9 mM Aβ(12−28) in 10 mM acetate-d_3 buffer in D_2O at pH 5.0. The peptide was dissolved at 5 °C and spectra A−C were recorded at 5 °C, 25 °C and 45 °C. Spectrum D was recorded at 25 °C after the sample had been kept for 1 h at 45 °C. Spectra were recorded using 1.5 s low-power water presaturation and are referenced to internal TSP. The assignments to particular amino acid residues are labeled using single letter notation. The S26 β proton resonance is also included.

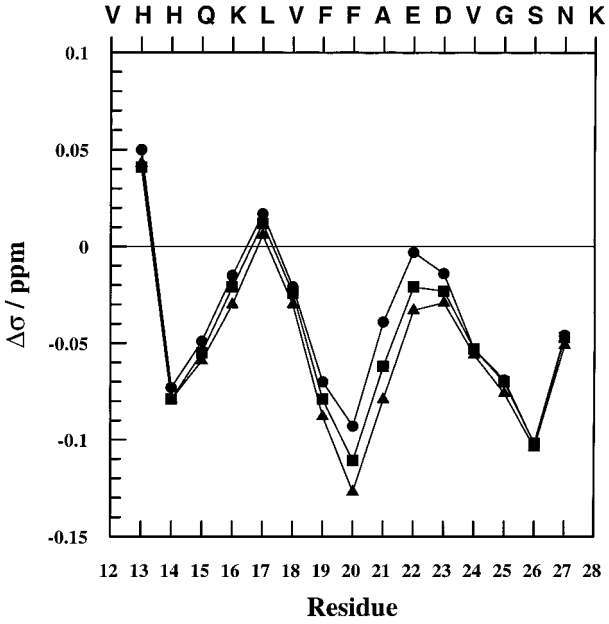

Figure 3. Temperature-induced α-proton secondary chemical shift changes of Aβ(12−28) from the spectra of Figure 2. Secondary chemical shifts at (●) 5 °C, (■) 25 °C, and (▲) 45 °C. The shifts were calculated relative to values for random coil conformation[32] and averaged over three neighboring residues. Proton chemical shifts are referenced using internal TSP at each temperature.

Figure 3 shows the secondary chemical shifts, calculated relative to random coil shifts[31] and averaged over three neighboring residues, of the α-protons along the peptide sequence at the three temperatures. In general, all α-proton shifts are close to those of random coil. However, small positive deviations from random coil shifts are seen, and the direction of the shifts are toward β-sheet secondary structure.[32] Figure 3

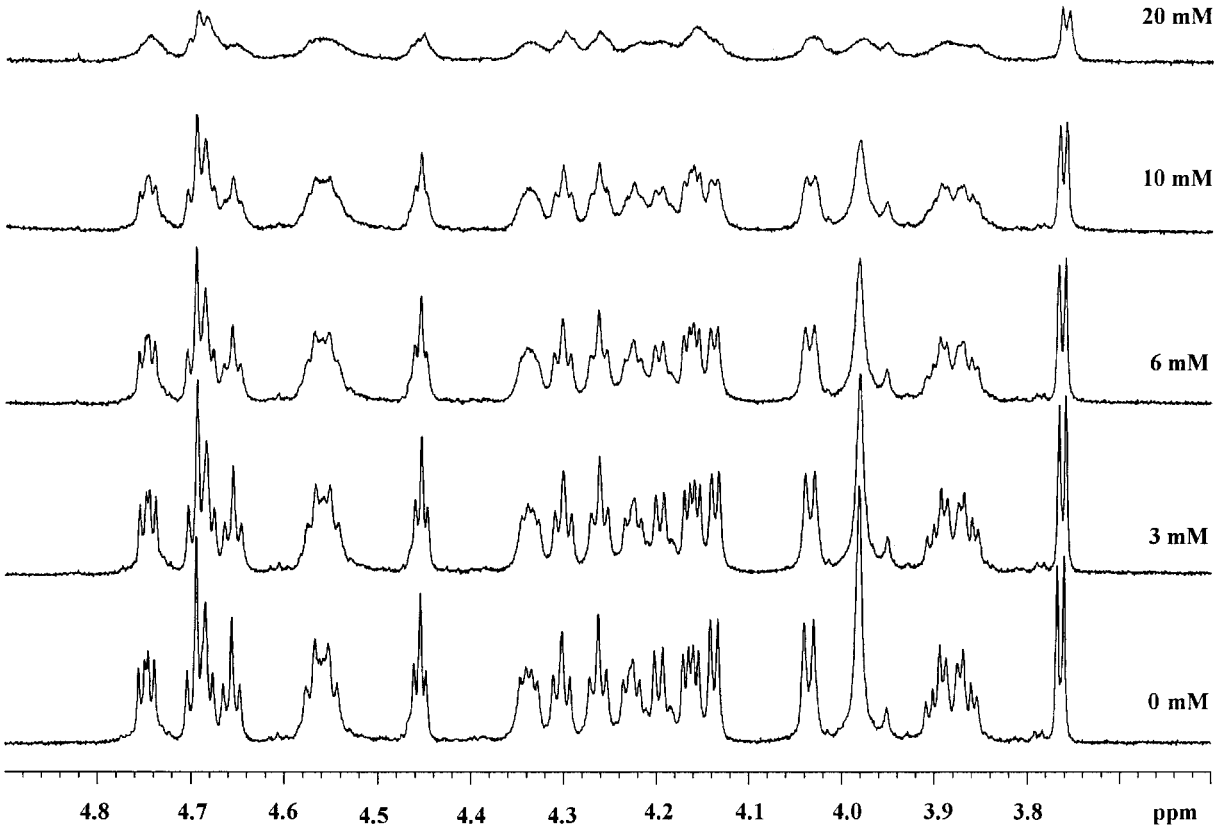

Figure 4. 800 MHz ^{1}H NMR spectra (α-proton region) of 1.0 mM Aβ(12−28) in 10 mM acetate-d_3 buffer in D_2O at pH 5.0. The spectra were recorded at 25 °C with addition of 0, 3, 6, 10, and 20 mM KF.

shows that at the higher temperatures most chemical shifts change further toward positive values, particularly those of residues F_{20}, A_{21}, and E_{22}, which shift another 0.03−0.05 ppm toward standard values for β-sheet[32] at 45 °C, compared to 5 °C. Increasing the ionic strength of the sample at 5 °C produced similar broadening of the resonances as were seen in the low ionic strength spectrum at 45 °C. Adding 20 mM KF gave a badly resolved NMR spectrum, where the individual resonance intensity had decreased significantly compared to the low salt spectrum (Figure 4). In this experiment, however, no detectable changes in the secondary α-proton chemical shifts were found to accompany the broadening of the resonances.

NMR Diffusion Experiments. Pulsed-field gradient NMR experiments were performed on the 0.9 mM Aβ(12−28) sample in D_2O buffer, pH 5.0 at 5, 25, and 45 °C. As shown in Figure 5, monoexponential curves were obtained at all three temperatures when the resonance intensity was plotted against the square of the gradient amplitude according to eq 1 (Experimental Section). The translational diffusion coefficients D_t are shown in Table 2. To compare the aggregational state of the NMR visible fraction at different temperatures, hydrodynamic radii were calculated from the diffusion coefficients employing the Stokes−Einstein relationship (eq 2). The solvent viscosity at different temperatures was approximated by D_2O viscosity.[33] The results are shown in Figure 6. No significant changes of the apparent hydrodynamic radius around 12 Å characterizing the NMR visible fraction were observed over the temperature range studied.

We also measured the diffusion of the KKLVFFA fragment itself and of its equimolar mixture with Aβ(12−28). The diffusion coefficients in the mixed sample were (3.1 and 1.7) $\times$ 10^{-10} m^2 s^{-1} for KKLVFFA and Aβ(12−28), respectively, at 25 °C, almost identical to the results from measurements on separate samples of the two peptides, under identical conditions.

NMR Studies of a Low Molecular Weight Fraction. Spectral observations: The 0.9 mM Aβ(12−28) sample was passed through a 30 kD filter at 25 °C, and the low molecular weight fraction without the highly aggregated part was collected and studied by NMR. A well-resolved spectrum was observed at 45 °C (Figure 7A). When the temperature was lowered to 5 °C after 18 h at 45 °C somewhat broader resonances were observed (Figure 7B), a temperature dependence at complete variance with the observations in Figure 2. In the nonfiltrated sample (Figure 2) the larger line widths at higher temperatures suggest a temperature-induced aggregation. In the filtrated sample, we observe the larger line widths at the lower temperature, a normal effect of lower molecular mobility at the lower temperature. However, the observed secondary chemical shifts observed at different temperatures (see particularly the α-proton resonance of A_{21} at 4.20 ppm at 5 °C) remain the same and are reversible in both cases, indicating that this is an inherent property of the low molecular weight fraction.

Diffusion Studies. A diffusion experiment at 25 °C on the sample passed through the 30 kD filter gave a diffusion coefficient of 1.77 $\times$ 10^{-10} m^2 s^{-1}, within the limit of uncertainty (5%) the same as the result obtained for the sample before filtration (Table 2). To study the effects of even more restrictive cutoff filtering, we then measured diffusion on a 0.4 mM sample passed through a 10 kD filter. At pH 5.0 and 25 °C, this sample gave a diffusion coefficient of 1.73 $\times$ 10^{-10} m^2 s^{-1}. The pH value of this sample was then adjusted to 2.9 (by

(32) Wishart, D. S.; Sykes, B. O.; Richards, F. M. *J. Mol. Biol.* **1991**, *222*, 311−333.

(33) Mills, R *J. Phys. Chem.* **1973**, *77*, 685−688. Kirshenbaum, I. *Physical Properties and Analysis of Heavy Water*; Urey H. C., Murphy G. M., Eds.; McGraw-Hill: New York, 1951.

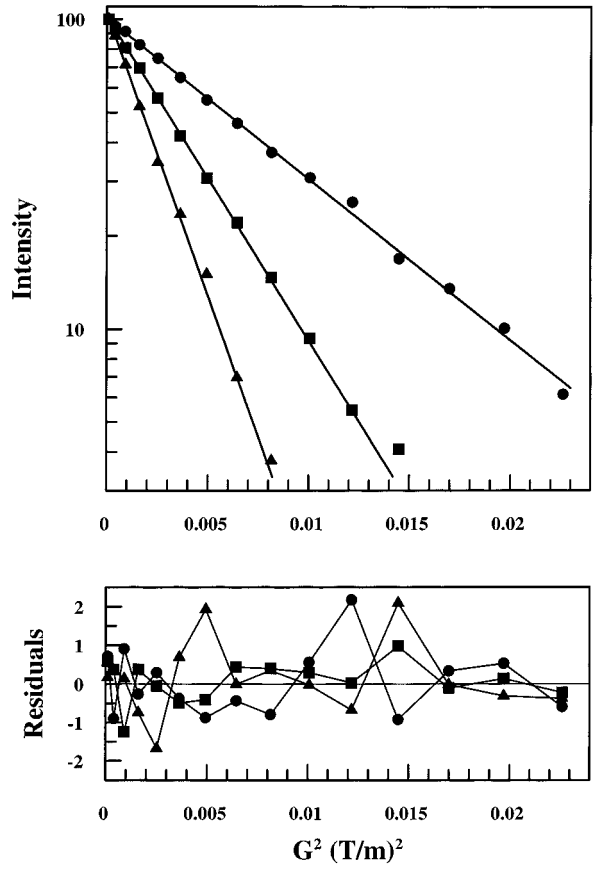

Figure 5. Pulsed-field gradient NMR diffusion experiments using 0.9 mM Aβ(12−28) in 10 mM acetate-d_3 buffer in D_2O at pH 5.0. Methyl resonances between 1.05 and 0.75 ppm were integrated and fitted to the Stejskal−Tanner equation (eq 1). (A) Series of diffusion experiments at (●) 5 °C, (■) 25 °C, and (▲) 45 °C. (B) Residuals relative to eq 1.

Table 2. Translational Diffusion Coefficients D_t for Aβ(12−28) in 10 mM Acetate-d_3 Measured by NMR under Various Conditions: Measurement Precision Is Ca 5%

sample concentration (mM)	temperature (°C)	pH	mol. wt cutoff filtration	$D_t \times 10^{10}$ ($m^2\,s^{-1}$)
	5	5.0	none	0.85
0.9	25	5.0	none	1.75
	45	5.0	none	2.9
0.6	25	5.0	<30 kD	1.77
0.4	25	5.0	<10 kD	1.73
0.4	25	2.9	<10 kD	1.67

adding HCl) in order to minimize any remaining aggregation. The measured diffusion coefficient was then again 1.67×10^{-10} $m^2\,s^{-1}$, not significantly different from the coefficient measured under our regular condition at pH 5.0.

Discussion

The NMR spectra of 0.9 mM Aβ(12−28) at pH 5.0 (corresponding to a pD of 5.4; cf. Experimental Section) show broader resonances toward the higher temperatures (Figure 2). This effect could be due to either intermediate chemical exchange with an NMR invisible fraction associated with very high molecular weight complexes and/or larger NMR observable aggregate sizes, and hence slower dynamics and shorter T_2. By visual inspection, the sample at 45 °C exhibited an increased viscosity, a preliminary indication of aggregation and β-sheet formation[34] under these conditions.

The results of the diffusion measurements (Figure 5, line width Table 1) and the molecular cutoff filtering (Table 1)

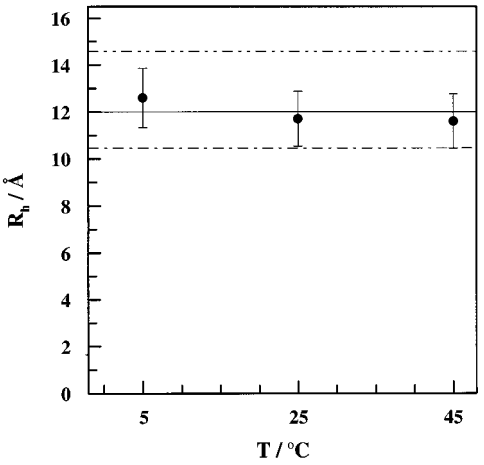

Figure 6. Effective hydrodynamic radii of the NMR visible fractions of Aβ(12−28) at different temperatures. The radii were calculated from the experimentally determined diffusion coefficients employing the Stokes−Einstein relationship (eq 2). The shape factor F was set to unity. The solvent viscosity at different temperatures was approximated by D_2O viscosity. The solid line corresponds to the average radius. The figure also shows the corresponding effective radii of monomeric [G[19,20]] Aβ(12−28) (− •) and dimeric [C[20]] Aβ(12−28) (− • •) forms of Aβ-(12−28) mutants, based on the Stokes−Einstein relationship and the experimental study by Mansfield et al..[15] The error bars represent 10% uncertainty, 5% from measured diffusion coefficients and 5% estimated from other sources (F, η in eq 2).

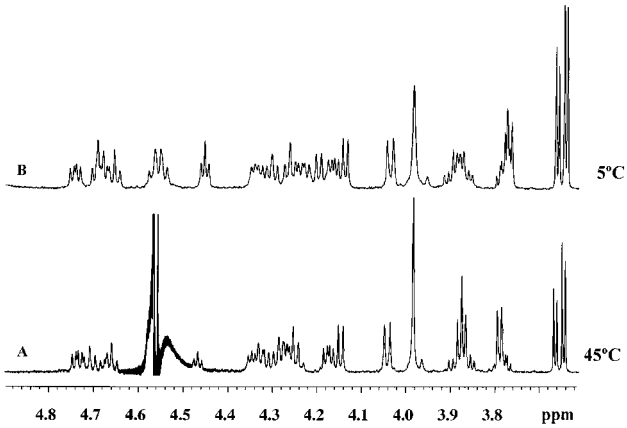

Figure 7. 600 MHz ^{1}H NMR spectra (α-proton region) of a low molecular weight fraction of Aβ(12−28). The sample was 0.6 mM in concentration after 0.9 mM Aβ(12−28) had been filtrated through a 30 kD molecular weight cutoff filter at 25 °C. Spectrum A was recorded at 45 °C. Spectrum) was recorded at 5 °C after the sample had been kept for 18 h at 45 °C. Remaining traces of glycerol from the cutoff filter are seen in spectra at 3.8 to 3.6 ppm and in B the remaining HDO signal around 4.55 ppm.

indicate that the reversible NMR line broadening towards the higher temperatures are mainly caused by increased presence of a larger fraction of high molecular weight aggregates, although some exchange effects cannot be excluded. The NMR time scale for intermediate chemical exchange of the α-protons is on the order of milliseconds at 800 MHz.[35] The time scale of the diffusion measurements is about 100 ms. Hence the influence of any temperature-dependent chemical

(34) Aggeli, A.; Bell, M.; Boden, N.; Keen, J. N.; Knowles, P. F.; McLeish, T. C. B.; Pitkeathly, M.; Radford, S. E. *Nature* **1997**, *386*, 259−262.

(35) From the expected chemical shift differences for H_α resonances between random coil and β-sheet secondary structure (ca 0.4 ppm, i.e., 320 Hz in an 800 MHz spectrometer) the characteristic time for intermediate exchange is $1/(2\pi 320) = 0.5$ ms.

exchange on the ms time scale between aggregates of different sizes should be rapid on the diffusion time scale and show up, for example, as a difference in diffusion constants for a sample before and after passage through a 30 kD filter or as a temperature-dependent hydrodynamic radius (Figure 6), in contrast to the observations. The measurements of the diffusion coefficients under varying conditions (Table 2) gave identical results. This observation shows that only the most low molecular weight fraction contributes to the diffusion results.

The CD results show a considerable amount of β-sheet, increasing at higher temperatures (Table 1). Similar CD spectral shapes due to concentration induced changes, but at a constant temperature, have been previously observed in Aβ(25−35).[36] These findings indicate that an NMR invisible fraction is in a dominating β-sheet conformation under the conditions used. Its aggregation state is heterogeneous, but the molecular weights are generally below 100 kD (corresponding to about 50 peptides). However, the results in Table 1 also indicate that the β-sheet structure is not fully developed in all aggregates. For instance, at 5 °C, about 50% of the peptide is in aggregates with molecular weights exceeding 10 kD, but the β-sheet secondary structure component is only 30%, significantly less than the aggregated fraction. The CD spectrum for Aβ(12−28) at 5 °C was the same before and after the sample had been kept for 30 min at 25 °C (Figure 1B, dashed line). This shows that the temperature-dependent change of the secondary structure, from the random coil toward a β-sheet like structure, is reversible after moderate temperature variations.

The temperature induced changes in secondary chemical shifts indicating the presence of more β-sheet like secondary structure are not directly related to the NMR line width effects and hence aggregation. This is shown by the NMR experiments on the sample that had been passed through a molecular weight cutoff filter. This procedure which removed all aggregates with molecular weight above 30 kD caused another line width behavior, in that no line broadening took place at 45 °C. The temperature induced changes in the chemical shifts of the α-protons were however identical to the changes in a nonfiltered sample (compare Figures 2 and 7). The chemical shift effects are therefore a property of the low molecular weight fraction itself. The shift changes are most pronounced for the residues 20−22, and suggest that their conformational space is not random but preconditioned toward dihedral angles corresponding to a more β-sheet like conformation at the higher temperatures.

Size exclusion chromatography (SEC) has been applied in order to determine the size of Aβ peptide aggregates.[6,7,8,28] We have also tried this technique under various conditions. We only observed a single size species passing the chromatography column. In comparison with the (linear) calibration curve it then seemed as if Aβ(12−28), as well as Aβ(1−40), was not in a monomeric state. However, when the concentration was varied (between 0.001 and 1 mM) no new peaks appeared in the chromatogram (data not shown). We concluded that the SEC technique is not reliable for the study of oligomerization in the case of small hydrophobic peptides. Other studies have led to similar conclusions.[8]

What is the dominating state of the low molecular fraction that we observe by NMR? The diffusion coefficient for Aβ(12−28) measured here is 1.75×10^{-10} m^2 s^{-1} in D_2O at 25 °C and pH 5.0, and almost the same at lower concentrations after filtration and at pH 2.9 (Table 2). As explained in the Experimental Section, the diffusion coefficients for representative monomeric and dimeric forms of 0.9 mM Aβ(12−28) should be (1.94 and 1.39) $\times 10^{-10}$ m^2 s^{-1}, respectively, in pure D_2O (based on data in ref 15; the recalibration of diffusion coefficients does not change the conclusions in that study). We conclude that the low molecular weight fraction of our 0.9 mM Aβ(12−28) sample at 25 °C is mainly in a monomeric state. A similar conclusion was also reached by Mansfield et al.[15] for their sample, measured down to 0.5 mM at pH 2.9. Recently a diffusion study (in 90% H_2O/10% D_2O) was reported, where it was suggested that a monomeric state should also exist with Aβ(1−40).[8] The diffusion coefficient for Aβ(1−40) ($D_t \sim 1.5 \times 10^{-10}$ m^2 s^{-1} at 25 °C) is in reasonable agreement with our monomeric diffusion coefficient for Aβ(12−28), considering the about 2.2 times higher molecular weight for Aβ(1−40) and the difference in viscosity (ratio 1.19) between the solvents.[37]

The monomeric form of Aβ(12−28) observed under the conditions employed by us is the major species giving rise to the NMR results. It has a dominating random coil structure with a tendency for its dihedral angles toward a more β-sheet like conformation, particularly at residues 20−22. Furthermore, it gives rise to the monoexponential diffusion curves in Figure 5. It is apparent from Figure 6 that the effective hydrodynamic radius R_h of the NMR visible fraction of Aβ(12−28) does not significantly change with temperature.[38] This is in contrast to the observed variation in NMR line widths when the temperature is varied. For comparison, Figure 6 also shows the effective radii for the known monomeric and dimeric mutants of the Aβ-(12−28) peptide, based on eq 2 and the diffusion coefficients given above from the measurements reported in ref 15. The agreement between the present result on Aβ(12−28) and the diffusion coefficient of the known monomer is reasonable.

The apparent domination of the monomeric state in the diffusion studies was unexpected, but may be explained by its expected faster diffusion and slower relaxation compared to the other NMR visible species at higher states of aggregation. Since the diffusion measurement is in principle a spin echo experiment, it will be biased in favor of the most slowly relaxing species in a mixture. The higher order aggregates therefore become invisible at the present level of precision in the diffusion measurements. Since there should be no fast chemical exchange between the monomer and the higher aggregates on the time scale of the diffusion measurements (100 ms), the increasing amount of (partly aggregated) β-sheet structure at the elevated temperatures is not reflected in the present diffusion experiments.

We observed that the two peptides KKLVFFA and Aβ(12−28) in a 1:1 mixture diffused independently of each other. This is in agreement with the filtering experiments, where a cutoff filter could separate the two peptide components. Hence, our experiments give no direct evidence for a strong interaction between KKLVFFA and the Aβ(12−28) peptide under the present conditions. This has been suggested to exist with Aβ(1−40),[39] where under different conditions the amount of early very large aggregates, as observed by fluorescence correlation spectroscopy, was reduced in the presence of KKLVFFA.[40]

(36) Terzi, E.; Hölzemann, G.; Seelig, J. *Biochemistry* **1994**, *33*, 1345−1350.

(37) From eq 2 the predicted D_t for Aβ(1−40) in 90% H_2O/10% D_2O is (1.75×10^{-10}) $(1.19 \cdot 2.2^{-1/3}) = 1.6 \times 10^{-10}$ m^2 s^{-1}.

(38) The calculated value of 12 Å for the effective hydrodynamic radius R_h is in reasonable agreement with a monomeric peptide with a normal hydration layer.

(39) Tjernberg, L. O.; Lilliehöök, C.; Callaway, D. J.; Näslund, J.; Hahne, S.; Thyberg, J.; Terenius, L.; Nordstedt, C. *J. Biol. Chem.* **1997**, *272*, 12601−12605.

(40) Tjernberg, L. O.; Pramanik, A.; Björling, S.; Thyberg, P.; Thyberg, J.; Nordstedt C.; Berndt, K. D.; Terenius, L.; Rigler, R. *Chem. Biol.* **1999**, *6*, 53−62.

The results observed at higher ionic strengths suggest that large aggregate sizes are a major reason for the salt-induced dependent increased NMR line width and loss of signal intensity. No chemical shift changes were observed along with the line broadening (Figure 4). The salt-induced β-sheet formation revealed by the CD spectra (Figure 1S) which is also in agreement with previous observations[41,42] is therefore completely invisible by NMR. The molecular cutoff filtering results also indicate the presence of very large molecular weight aggregates already at low peptide concentrations, at high salt concentrations. We suggest that the addition of salt (∼100 mM KF) to the 0.9 mM Aβ(12−28) sample gives directly rise to large aggregates, due to a hydrophobic collapse, with hardly any detectable low molecular weight fraction. Under these conditions we could not measure diffusion due to the fast proton relaxation rate.

At the present stage our systems give no evidence for an α-helical structure, which has been shown to be stabilized in a solvent mixture, including detergent micelles and phospholipid membranes.[43] Interestingly, a slowly emerging transitory α-helical component, in parallel with a random coil to β-sheet transition, was recently reported[10] to exist upon prolonged (weeks) incubation of so-called low molecular weight Aβ(1−40). This process was taking place in vitro (buffer alone) and resulted in protofibrils and terminal fibrils. Protofibrils were shown to be in continuous equilibrium with low molecular weight entities.[43] It is not known whether this intermediate α-helical structure is induced in an aggregated environment.

The observed temperature dependence of the equilibrium between the low molecular weight fraction (in a dominating random coil state) and the larger aggregates (with dominating β-sheet structures) indicates that the aggregation and β-sheet assemblies are driven mainly by hydrophobic interactions. Electrostatic effects are observable as a repulsive effect under low ionic screening (and a pH distant from the pI ∼6), which counteracts the aggregation and instead promotes the monomeric state and a random coil secondary structure. The aggregation process in certain respects resembles protein folding, and the disaggregation process the cold denaturation of proteins. The formation of the aggregates is likely to be strongly cooperative under the conditions used here. At present, we have no information about any critical concentration (cf. cmc) of the peptide aggregation, similar to that observed for Aβ(1−40).[3]

The present study on Aβ(12−28) and the one reported[8] on Aβ(1−40) were both carried out with nonphysiologically high peptide concentrations. It is interesting, however, to note that even with an extreme concentration, a large proportion of the Alzheimer peptides can initially be in a monomeric state, although only as a metastable one. Under these in vitro conditions, monomeric and oligomeric states will probably participate in the formation of protofibrils, the precursors of fibrils with their amyloidic β-sheet structure. The AD is manifested by the plaques (amyloid) deposition, where the growth of plaques onto an AD cortex specimen was found to be mediated by the deposition of Aβ peptides in their monomeric state.[1,8] The original amyloid hypothesis about neuorotoxicity has recently been reexamined and challenged.[44] Also small oligomeric Aβ aggregates have been reported to be potent neurotoxins.[45]

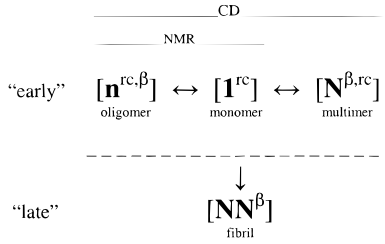

Figure 8. Suggested scheme for the equilibria and aggregational states observed in vitro with the Aβ(12−28) peptide at mM concentration in low ionic strength buffer at pH 5.0. A monomeric state [1] with a dominating random coil (rc) structure is in equilibrium with heterogeneous oligomeric states [n] with a mixed random coil/β-sheet structure. Invisible by NMR but observable in the CD spectra, there are heterogeneous larger aggregates or multimers [N] with a dominating β-sheet structure. These may be considered as protofilaments. Temperature induced reversible transitions were observed in this study between [1], [n], and [N], and the average aggregate size as well as the degree of β-sheet increase with temperature. After the "early" events amyloidic fibrils, [NN], may be formed at a "late" stage (not studied here), primarily from protofilaments and monomers.

Conclusions

The present study deals with early events of the fibrillogenesis process, before fibrils (plaques) will assemble. High ionic strength promotes aggregation and β-sheet formation in the Aβ(12−28) peptide. From the observations of the temperature induced changes in secondary structure in a low ionic strength sample we suggest a simple in vitro scheme for the aggregation and secondary structure conversion (Figure 8). In this scheme, a certain fraction of Aβ(12−28) is in monomeric state with a dominating random coil conformation. The monomers are in equilibrium with heterogeneous fractions of aggregates of various sizes, and these are partly in β-sheet conformation. Those with the highest molecular weights are not observed by NMR, but only by CD spectroscopy. At elevated temperatures, the monomers, and particularly their central hydrophobic segment, may be in a conformation with a preference for β-strand like dihedral angles.[46] As the sizes of the multimers (which may be considered as protofilaments) increase with temperature, a further, initially reversible conversion to β-sheet takes place.

Experimental Section

Materials. Alzheimer β-peptide fragments Aβ(12−28) and the KKLVFFA were purchased from Neosystem Lab., Strasbourg. The purity of peptides was tested by HPLC, MS, and NMR. β-cyclodextrin was purchased from Sigma-Aldrich. The quantities of solid materials for all samples were determined by weight.

NMR Spectroscopy. The samples for NMR experiments were prepared at a concentration of 0.9 mM of Aβ (12−28) by directly dissolving solid material in 99.95% D_2O buffered by 10 mM sodium acetate-d_3. This was carried out at 5 °C unless otherwise specified. The pH was measured with a combination glass microelectrode, designed for NMR (Orion model 9826BN, with model 320 pH meter). Unless otherwise stated, all the pH values are *uncorrected* meter readings. For samples dissolved in D_2O, a correction of +0.4 units

(41) Hilbich, C.; Kisters-Woike, B.; Reed, J.; Masters, C. L.; Beyreuther, K. *J Mol. Biol.* **1991**, 218, 149−63.

(42) Snyder, S. W.; Ladror, U. S.; Wade, W. S.; Wang, G. T.; Barrett, L. W.; Matayoshi, E. D.; Huffaker, H. J.; Krafft, G. A.; Holzman, T. F. *Biophys. J.* **1994**, 67, 1216−28.

(43) Ma, K.; Clancy, E. L.; Zhang, Y.; Ray, D. G.: Wollenberg, K.; Zagorski, M. G. *J. Am. Chem. Soc.* **1999**, *121*, 8698−8706.

(44) Neve, R. L.; Robakis, N. K. *Trends Neurosci.* **1998**, *21*, 15−19.

(45) Lambert, M. P.; Barlow, A. K.; Chromy, B. A.; Edwards, C.; Freed, R.; Liosatos, M.; Morgan, T. E.; Rozovsky, I.; Trommer, B.; Viola, K. A.; Wals, P.; Zhang, C.; Finch, C. E.; Krafft, G. A.; Klein, W. L. *Proc. Natl. Acad. Sci.* **1998**, *95*, 6448−6453.

(46) After the submission of the present manuscript, a CD study was reported on the temperature dependence of solutions of Aβ(1−40) in water at pH 4.6 (Gursky O.; Aleshkov S. *Biochim. Biophys. Acta* **2000**, *1476*, 93−102). Their results and interpretation on the longer peptide are in accordance with the present conclusions based on NMR and CD on the 1 order of magnitude more concentrated solutions of Aβ(12−28).

should be added to the readings in order to get a corresponding pD value.[47] Under these conditions, the NMR spectra were resolved and the samples were stable over a period of several weeks, provided that the storage was at a low temperature. NMR measurements were performed using 5 mm tubes and standard pulse sequences on Varian Inova 600 and 800 MHz spectrometers. Secondary chemical shifts were calculated using reported random coil chemical shifts (see Table 6 in ref 31).

Molecular Weight Cutoff Filtering. Centricon concentration filters (Amicon, Inc., Beverly, MA) with cutoff at 3−100 kD were used. The filters are specified by manufacturers to give typically 90−95% passage of various biomolecules with a molecular weight well below the cutoff limit. The filters were cleaned from glycerol by washing with buffer and centrifugation four times. All samples were diluted in a 10 mM acetate buffer, pH 5.0, and kept at 5 °C until centrifugation. This was carried out at 4125*g* for 10 min at 5, 25, and 45 °C (Centrifuge 5403, Eppendorf). To estimate the retention of a particular sample in a filter, aliquots of (20 μL) of the samples, before and after filtration, were analyzed in terms of relative concentrations. The analysis was performed by HPLC (Shimadzu LC-10A) using a gel filtration column (Superose 12 HR 10/30, Pharmacia). The absorbance was measured at 214 nm with a Shimadzu SPD-10A unit. The mobile phase was 70 mM NaP_i buffer at pH 5.6 with 150 mM KF. The flow rate was 0.4 mL/min. The gel filtration column was also calibrated for size exclusion chromatography (SEC) using various relevant molecular weight markers.

CD Spectroscopy. A JASCO J-720 spectropolarimeter and a PTC-343 temperature controller were employed. The spectral range was 190−250 nm with a resolution of 0.2 nm and a bandwidth of 1 nm. A scan speed of 100 nm/min with 2 s response time was usually employed. Cells with optical paths 0.05−10 mm were used. Since a high concentration of NaCl has high absorbance in the UV-region, we instead used KF in the salt effect experiments. The spectral contribution from the background was subtracted and the results were expressed as mean residue molar ellipticity [θ]. The evaluation of secondary structure content was based on comparison with standard CD spectra as previously described.[48]

NMR Diffusion Experiments. The signal intensity I recorded in the PFG NMR experiment is given by the Stejskal−Tanner equation:[49]

$$I = I_o \exp[-\gamma^2 G^2 D_t \delta^2 (\Delta - \delta/3)] \quad (1)$$

Here I_o is the signal intensity in the absence of gradients, D_t is the diffusion coefficient for unrestricted translational diffusion of a molecule in an isotropic medium, γ is magnetogyric ratio of the nucleus measured (for protons $\gamma_H = 26.752 \times 10^7$ rad T^{-1} s^{-1}), G is the magnitude, and δ is the duration of the field gradient, and Δ is the longitudinal storage period. D_t was evaluated from the curves based on eq 1 with an estimated precision of 5%.

At high dilution, the translational diffusion coefficient D_t will be related to the molecular hydrodynamic radius R_h according to the Stokes−Einstein equation:

$$D_t = \frac{k_B T}{6\pi\eta R_h F} \quad (2)$$

where k_B is the Boltzmann constant, T is the absolute temperature, η is the viscosity, and F is a shape factor.[50] From the experimentally determined radius R_h, the molecular weight M of the particle can be estimated, assuming a partial specific volume and a hydration layer. In the first approximation $R_h \propto M^{1/3}$.

The gradient strength was calibrated using a residual proton signal in 99.95% D_2O and a literature value of 1.90×10^{-9} m^2 s^{-1} for the HDO translational diffusion coefficient.[33]

For representative monomeric and dimeric forms of 0.9 mM Aβ(12−28) at 25 °C and pH 2.9, the reported[15] values are (2.48 and 1.78) $\times 10^{-10}$ m^2 s^{-1}, respectively. Mansfield et al.[15] calibrated their magnetic field gradients based on a reported[51] literature value (3.24×10^{-10} m^2 s^{-1} at 25 °C) for the diffusion coefficient of β-cyclodextrin, which had been dissolved in a 100% H_2O medium. However, their NMR studies of diffusion were made in D_2O. In an attempt to calibrate the diffusion coefficient measured by us for Aβ(12−28) on an absolute scale, we measured the diffusion coefficients for β-cyclodextrin at 25 °C in 100% D_2O as well as in 90% H_2O/10% D_2O and found them to be (2.53 and 3.05) $\times 10^{-10}$ m^2 s^{-1}, respectively. The viscosity of pure D_2O is 1.21 times that of pure H_2O at 25 °C,[33] or 1.19 times that of 90% H_2O/10% D_2O. The 1.20 ratio between the two diffusion coefficients measured by us for β-cyclodextrin is obviously close to that expected for the two solvents from the different viscosities. The diffusion coefficient for β-cyclodextrin in 90% H_2O/10% D_2O determined by us is also in reasonable agreement with the above-mentioned literature[44] value 3.24×10^{-10} m^2 s^{-1} (in pure H_2O). Using the new value for β-cyclodextrin measured by us in 100% D_2O as a calibration, we estimate the diffusion coefficients of Aβ(12−28) monomers and dimers in pure D_2O at 25 °C to be (1.94 and 1.39) $\times 10^{-10}$ m^2 s^{-1}, respectively, from the values given in ref 15.

Acknowledgment. We thank Maria Assarson for performing preliminary experiments with size exclusion chromatography. This work was supported by grants from the Swedish Natural Science Research Council, the Swedish Alzheimer Foundation and the Carl Trygger Foundation. A fellowship to J.J. from the Swedish Royal Academy of Sciences is gratefully acknowledged. We thank the Swedish NMR Center in Göteborg for access to the 800 MHz NMR spectrometer.

Note Added in Proof. We have determined the diffusion coefficient of [$G^{19,20}$] Aβ (12−28), 0.9 mM in 10 mM sodium acetate-d_3 in D_2O, pH 5.0, 25 °C and found $D_t = 1.90 \times 10^{-10}$ m^2 s^{-1} for this monomer form, in good agreement with the estimate from ref 15.

Supporting Information Available: Circular dichroism spectra of 0.9 mM Aβ(12−28) in the presence of 2, 6, 10, and 20 mM KF. 800 MHz ^{1}H NMR spectra (α-proton region) of 0.9 mM Aβ(12−28) with 40 h interval (PDF). This material is available free of charge via the Internet at http://pubs.acs.org.

JA991167Z

(47) Glasoe, P. K.; Long, F. A. *J. Phys. Chem.* **1960**, *64*, 188−190.
(48) Greenfield, N.; Fasman, G. *Biochemistry* **1969**, *8*, 4108−4116.
(49) Stejskal, E. O.; Tanner, J. E. *J. Phys. Chem.* **1965**, *42*, 288−292.
(50) Cantor, C. R.; Schimmel, P. R. *Biophysical Chemistry, Part II*; W. H. Freeman and Company: San Francisco, 1980; Chapter 10.
(51) Uedaira, H.; Uedaira, H. *J. Phys. Chem.* **1970**, *74*, 2211−2214.